Multicomponent nucleation and droplet growth in natural gas

Multicomponent nucleation and droplet growth in natural gas

C. C. M. Luijten and R. G. P. van Hooy
Department of Applied Physics, Eindhoven University of Technology, P.O. Box 513, 5600 MB Eindhoven, The Netherlands

J. W. F. Janssen
Gasunie Research, P.O. Box 19, 9700 MA Groningen, The Netherlands

M. E. H. van Dongen
Department of Applied Physics, Eindhoven University of Technology, P.O. Box 513, 5600 MB Eindhoven, The Netherlands

(Received 13 March 1998; accepted 28 May 1998)

The first quantitative experimental results are presented on homogeneous nucleation and droplet growth in a multicomponent gas-vapor mixture. Using the pulse-expansion wave tube technique, we investigated the condensation behavior of natural gas consisting of over 30 components. Data were obtained in the pressure range between 6 and 24 bar and at temperatures ranging from 221 to 237 K. The observed droplet growth rates are quantitatively explained using a multicomponent model for diffusion controlled growth. The nucleation rate data are for the moment mainly presented as a challenge to theoreticians, although some qualitative arguments are presented that could be helpful in the interpretation. The data appear to agree at least qualitatively with theoretical values (according to the revised binary classical nucleation theory) for a mixture of *n*-octane and methane, a model mixture which also shows the same macroscopic phase behavior as natural gas. © *1998 American Institute of Physics.* [S0021-9606(98)50733-7]

I. INTRODUCTION

Since quantitative nucleation rate measurements became possible, there has been interest not only in the nucleation behavior of single substances, but also in that of binary and even ternary[1] mixtures. To our present knowledge, no nucleation rates have ever been determined for more comprehensive systems, although onset points for natural gas (consisting of more than 40 components) were measured by Muitjens *et al.*[2]

The interest of the latter authors in natural gas condensation not only resulted from a fundamental interest in multicomponent nucleation, but there were also practical considerations: uncontrolled condensation of the numerous heavy hydrocarbons present in natural gas would have its impact on industrial gas transport. Therefore, these hydrocarbons are removed from the flow by inducing a controlled dropwise condensation process, followed by separation of the resulting droplets.

In order to design more efficient procedures for this removal process, quantitative knowledge is required about the nucleation and growth of the droplets in the natural gas. This application, together with the (at first instance open) question whether or not it would be possible to obtain quantitative data for such a complicated mixture, led us to investigate the condensation behavior of natural gas.

For this investigation use was made of our pulse-expansion wave tube facility, in which nucleation and droplet growth are separated in time by the well-known nucleation pulse method. Since the tube was specially designed for use at moderate pressures, data could be obtained for realistic gas transport conditions of several tens of bars. Special effort was made to assure that the composition of the gas (determined separately) was kept constant during the preparation stage of the experiments.

The observed nucleation rates are compared to an existing multicomponent nucleation model.[3] The agreement is not very satisfactory, and possible reasons for this observation are discussed. The droplet growth rates can be quantitatively accounted for by assuming diffusion controlled growth for the case of multiple diluted vapors in a noncondensible gas.

II. EXPERIMENTAL PROCEDURE

The experimental setup used for nucleation and growth experiments has been described in various earlier papers.[4–7] The required nucleation pulse is generated by gas dynamic waves propagating in a modified shock tube; the resulting—monodispersed—droplet population is observed using a combination of constant angle Mie scattering and extinction measurement.

The experiments described here differ from earlier ones with respect to the preparation of the gas-vapor mixture. Usually, the test mixture is prepared in the high pressure section of the wave tube (HPS) by mixing a vapor component with a carrier gas. In the present work, however, the natural gas was received in cylinders that had been filled directly from the Dutch natural gas distribution system. These cylinders contained all components originally present in the natural gas, except for water vapor (which had been extracted by the production company at an earlier stage). Therefore, it was essential to bring this mixture into the HPS without altering its composition.

TABLE I. Natural gas compositions in terms of molar fractions y_i for each cylinder type. The i-components denote isomers of the respective alkanes.

Component	Type A	Type B	Type C
Methane	8.13E-1	8.13E-1	8.13E-1
Ethane	2.85E-2	2.84E-2	2.84E-2
Propane	3.95E-3	3.92E-3	3.92E-3
n-butane	7.31E-4	7.32E-4	7.25E-4
2-methylpropane	6.37E-4	6.43E-4	6.33E-4
n-pentane	1.62E-4	1.63E-4	1.60E-4
2-methylbutane	1.68E-4	1.69E-4	1.66E-4
2,2-dimethylpropane	7.20E-5	7.34E-5	7.21E-5
n-hexane	6.03E-5	6.06E-5	5.97E-5
3-methylpentane	2.14E-5	2.15E-5	2.12E-5
2,2-dimethylbutane	5.62E-5	5.73E-5	5.64E-5
2,3-dimethylbutane	3.56E-5	3.58E-5	3.51E-5
n-heptane	2.86E-5	2.88E-5	2.83E-5
i-heptane	4.38E-5	4.76E-5	4.70E-5
$(n+i)$-octane	3.30E-5	2.69E-5	3.23E-5
$(n+i)$-nonane	1.60E-5	1.40E-5	1.78E-5
$(n+i)$-decane	1.12E-5	1.11E-5	1.10E-5
$(n+i)$-undecane	2.60E-6	2.90E-6	2.90E-6
$(n+i)$-dodecane	2.00E-7	2.00E-7	2.00E-7
Benzene	1.77E-4	1.71E-4	1.67E-4
Toluene	3.96E-5	3.62E-5	3.95E-5
Xylenes	1.34E-5	1.33E-5	1.28E-5
Cyclopentane	1.30E-5	1.31E-5	1.31E-5
Cyclohexane	1.94E-5	2.02E-5	1.99E-5
Methylcyclohexane	2.46E-5	2.44E-5	2.41E-5
Helium	5.00E-4	5.00E-4	5.00E-4
Nitrogen	1.41E-1	1.42E-1	1.42E-1
Carbondioxide	9.90E-3	9.90E-3	9.90E-3

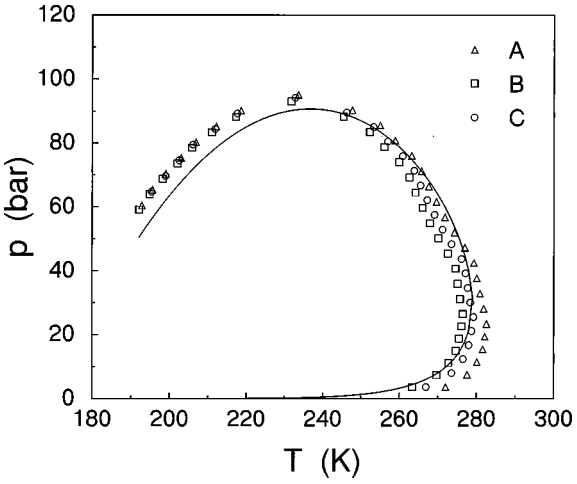

FIG. 1. Vapor-liquid coexistence envelopes for the natural gas under study, calculated using the SRK equation of state. Symbols refer to different gas cylinder types; the solid line is the SRK phase envelope for n-octane (molar fraction 5×10^{-4}) in methane.

Experiments were performed with three different types of gas cylinders—filled from the same supply—denoted as A, B and C. In order to reduce the decrease in reservoir pressure per experiment, we used three cylinders of each type in parallel, whereas one of each was used for composition analysis by a company with special analysis facilities for heavy hydrocarbon compounds (BEB GmbH, Hannover, Germany). The compositions of the gases are listed in Table I.

As a result of the presence of heavy hydrocarbons the natural gas shows retrograde phase behavior, implying that condensation can even take place upon isothermal pressure release from the container. The phase diagram for each of the gases used was calculated from several equations of state[8] using the PRO/II-package (Simulation Sciences Inc., Brea, CA). The resulting vapor-liquid coexistence envelopes for the Soave–Redlich–Kwong (SRK) equation are shown in Fig. 1, together with the phase diagram for an n-octane/methane mixture (see Sec. III). Phase envelopes calculated using the Peng–Robinson (PR) equation (not drawn in Fig. 1) are slightly shifted to the inner side with respect to the SRK envelopes.[9]

To prevent preliminary (retrograde) condensation due to large pressure drops between the cylinders and the test section, we applied the following procedure. First, the test section was filled with dry nitrogen up to the desired initial pressure value p_0. This value nearly equals the pressure remaining in the reservoir after a previous experiment, to prevent any pressure reduction at the cylinder exit. Then, the nitrogen was slowly and isobarically pushed out from the HPS by adding natural gas at one side (near the observation point), thereby simultaneously releasing the nitrogen over a needle valve at the other end of the test section and measuring the dispelled volume. Test runs, in which methane was pushed out by nitrogen and monitored using gas chromatography, indicated that it was sufficient to flush the total test volume three times in order to assure complete expulsion of the nitrogen.

It is assumed that, due to the careful isobaric flushing, any possible wall adsorption of heavy hydrocarbons is also equilibrated, thus leaving a test mixture with the same molar fractions as that in the reference cylinder used for analysis. As a final check, some experiments were given a sixfold flushing volume, but the results did not differ from the others. In the low pressure section (LPS) of the setup, a mixture of nitrogen and methane (with a molar ratio corresponding to that in natural gas) was used in order to achieve the best possible wave patterns.

Each series of experimental runs started with an expansion that was deliberately chosen too deep for a proper pulse experiment, but that did yield the onset pressure of condensation. The onset temperature was then calculated via conservation of entropy, using a Lee–Kesler-type equation of state for the full mixture. In the next experiment, the LPS pressure was then adjusted to give the proper pressure ratio between the nucleation pulse and the initial state, in order to situate the previously calculated onset temperature in the pulse. After a few trials, well-defined pulse experiments turned out to be possible.

As the experiments proceeded, both the reservoir pressure (determining p_0) and the total nucleation pressure continuously decreased. As a result, the nucleation behavior slightly changed, causing a need to shift to lower temperatures (our setup, like all others, has a limited range of observable nucleation rates). By slightly adjusting the imposed pressure ratio during a series, we were able to ''keep track''

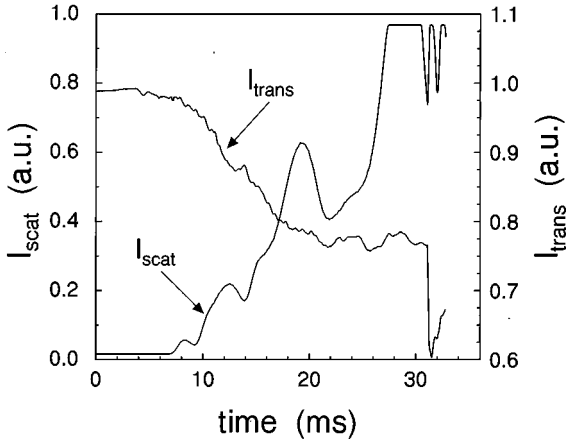

FIG. 2. Scattered and transmitted intensity for a representative experiment (run 307, see Tables II and III). Note the sudden changes due to the shock reflection at $t=31.1$ ms.

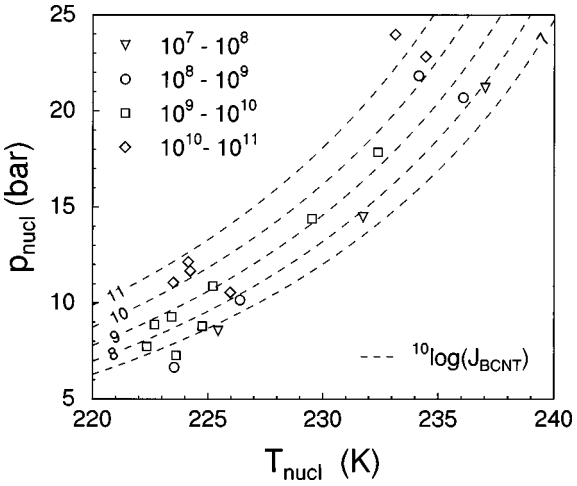

FIG. 4. Experimental data for natural gas in cylinder type A, represented in the (p,T) diagram. The nucleation rate classes are given in units of cm^{-3} s^{-1}. Dashed lines are isonucleation curves according to BCNT for *n*-octane (molar fraction 5×10^{-4}) in methane.

of a broader band of isonucleation curves, see Sec. III.

III. RESULTS AND DISCUSSION

In Fig. 2, the optical signals are shown for a representative nucleation experiment in natural gas. In spite of the enormous complexity of the mixture under study, the extrema in the scattered intensity (Mie peaks) can be remarkably well recognized. By comparison with the theoretical scattering for liquid droplets having an index of refraction of 1.405—a value that is representative for the heavier hydrocarbons—the droplet growth can accurately be determined. The fourth peak is out of the preset acquisition range; its moment of occurrence is estimated to be $t=29.0$ ms. The deduced droplet growth curve is plotted in Fig. 3 together with the pressure history, which may serve as a reference for the time axis. Note that the square of the radius increases linearly in time, with the start of vapor depletion being just visible at the end of the growth period.

The time-resolved droplet radius is used for deriving the droplet number density from the extinction, in a manner described before.[6] The relatively large noise on the transmitted signal (see Fig. 2) is not typical for the present multicomponent system; it is always observed at higher experimental pressures and must probably be ascribed to mechanical disturbances in the tube wall due to the wave propagation. However, some of the lower frequency oscillations—those with a period of about 4 ms, visible after $t\approx18$ ms—are also present in the theoretical curve.

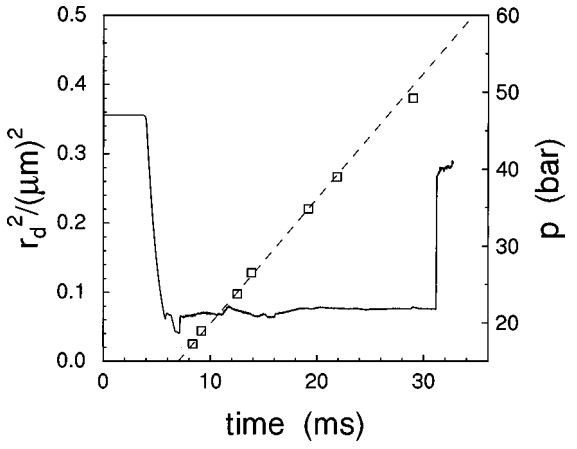

FIG. 3. Droplet radius squared and pressure as a function of time for the sample experiment (run 307, see Tables II and III). The dashed straight line is the best fit to quadratic growth.

A. Homogeneous nucleation

In Fig. 4, we present nucleation results for experiments with natural gas from cylinder type A. The data are grouped in classes, each of them covering one order of magnitude in nucleation rate. Although the isonucleation lines are not perfectly smooth, they do appear in the expected order: higher nucleation rates are observed when going in the direction of lower temperatures and higher pressures (that is, directed inwards the coexistence envelope, see Fig. 1).

Gas types B and C showed the same results as type A, even in a quantitative sense. For the sake of brevity, we will not reproduce the results here. We merely state that—apparently—the slight differences in composition (see Table I) do not significantly alter the nucleation behavior in the present range of conditions.

In Fig. 4, we also compare the experimental isonucleation curves with theoretical ones for a mixture of methane and *n*-octane (with a molar fraction $y=5\times10^{-4}$), in the same range of nucleation rates. The latter were calculated using (revised) binary classical nucleation theory (BCNT); details of these calculations—in which the thermodynamics are also based on the Soave–Redlich–Kwong equation of state—are extensively described elsewhere.[10] In the range of conditions investigated, the experimental nucleation rates appear to lie within approximately two orders of magnitude from the corresponding BCNT values for the binary model mixture.

The particular *n*-octane fraction of 5×10^{-4} was chosen to fit the macroscopic phase behavior of the natural gas: the coexistence envelope of the model mixture strongly re-

TABLE II. Lumped feed composition and equilibrium molar fractions (according to PR equation) for nucleation and growth conditions of a typical experiment (run 307). $T_{\mathrm{nucl}}=233.1$ K, $p_{\mathrm{nucl}}=14.8$ bar; $T_{\mathrm{grow}}=242.2$ K, $p_{\mathrm{grow}}=21.8$ bar. Individual contributions to the effective supersaturation are also given.

Component	$y_{i,\mathrm{feed}}$	$y_{i,\mathrm{nucl}}^{\mathrm{eq}}$	$x_{i,\mathrm{nucl}}^{\mathrm{eq}}$	$y_{i,\mathrm{grow}}^{\mathrm{eq}}$	$x_{i,\mathrm{grow}}^{\mathrm{eq}}$	S_i	$(S_i)^{x_{i,\mathrm{nucl}}^{\mathrm{eq}}}$
Methane	8.13*E*-1	8.13*E*-1	1.17*E*-1	8.13*E*-1	1.18*E*-1	1.00	1.000
Ethane	2.84*E*-2	2.84*E*-2	5.04*E*-2	2.84*E*-2	4.42*E*-2	1.00	1.000
Propane	3.92*E*-3	3.91*E*-3	3.94*E*-2	3.92*E*-3	3.15*E*-2	1.00	1.000
n-butane	1.38*E*-3	1.34*E*-3	6.48*E*-2	1.36*E*-3	4.73*E*-2	1.03	1.002
n-pentane	4.05*E*-4	3.68*E*-4	7.67*E*-2	3.90*E*-4	5.41*E*-2	1.10	1.007
n-hexane	1.75*E*-4	1.21*E*-4	1.10*E*-1	1.51*E*-4	8.49*E*-2	1.45	1.041
n-heptane	7.64*E*-5	2.91*E*-5	9.58*E*-2	4.89*E*-5	9.59*E*-2	2.63	1.097
n-octane	2.69*E*-5	1.63*E*-6	5.12*E*-2	5.13*E*-6	7.59*E*-2	16.5	1.154
n-nonane	1.40*E*-5	1.67*E*-7	2.80*E*-2	6.56*E*-7	4.65*E*-2	83.8	1.132
n-decane	1.11*E*-5	2.66*E*-8	2.24*E*-2	1.24*E*-7	3.82*E*-2	417	1.145
n-undecane	2.90*E*-6	2.01*E*-9	5.87*E*-3	9.94*E*-9	1.01*E*-2	1443	1.044
n-dodecane	2.00*E*-7	3.37*E*-11	4.05*E*-4	1.84*E*-10	6.96*E*-4	5935	1.004
Benzene	1.71*E*-4	8.53*E*-5	1.74*E*-1	1.27*E*-4	1.54*E*-1	2.00	1.129
Toluene	3.62*E*-5	5.33*E*-6	6.25*E*-2	1.32*E*-5	8.01*E*-2	6.79	1.127
m-xylene	1.33*E*-5	3.83*E*-7	2.62*E*-2	1.32*E*-6	4.17*E*-2	34.7	1.097
Cyclopentane	1.31*E*-5	1.06*E*-5	5.16*E*-3	1.20*E*-5	3.75*E*-3	1.24	1.001
Cyclohexane	2.02*E*-5	9.88*E*-6	2.09*E*-2	1.49*E*-5	1.85*E*-2	2.04	1.015
Methylcyclohexane	2.44*E*-5	5.73*E*-6	3.78*E*-2	1.21*E*-5	4.28*E*-2	4.26	1.056
Nitrogen	1.42*E*-1	1.42*E*-1	4.01*E*-3	1.42*E*-01	4.68*E*-3	1.00	1.000
Carbon dioxide	9.90*E*-3	9.90*E*-3	7.55*E*-3	9.90*E*-03	6.85*E*-3	1.00	1.000

sembles those of natural gas, see Fig. 1. The mere fact that the same observation holds for the isonucleation curves justifies studying binary methane/alkane mixtures as computational model systems for natural gas. We would like to stress that we are *not* claiming that BCNT correctly describes the nucleation of these mixtures; actually, previous experiments have shown quite large discrepancies.[3,5,11] Our point is that the BCNT calculations for these binaries can very well be used as a reasonable interpolation to mimic both the equilibrium *and* nonequilibrium (nucleation) behavior of the natural gas under study.

We also compared our data to the multicomponent nucleation model of Kalikmanov and Van Dongen.[3] The latter uses the concept of an effective supersaturation $\overline{S}$, defined as the product of partial saturations of the individual components raised to the power of their equilibrium molar fraction in the liquid:

$$\overline{S}=\prod_{i=1}^{n}\left(\frac{y_i}{y_i^{\mathrm{eq}}}\right)^{x_i^{\mathrm{eq}}}. \tag{1}$$

We implemented the multicomponent model as follows. First, using the compositions of Table I as input (feed), equilibrium flash calculations are performed using either the SRK or PR equation of state. At given p and T (nucleation or growth conditions), these calculations yield the equilibrium composition of both phases. Having obtained these vapor and liquid equilibrium fractions, we apply a lumping procedure: helium is taken together with nitrogen; alkane isomers are lumped with their corresponding straight-chain alkane, up to $C_{12}H_{26}$; cyclic hydrocarbons are considered separately. The results for one experiment with composition B (calculated using the PR-equation of state) are given as an example in Table II. Finally, for the resulting 20-component mixture, the nucleation rate is computed according to the model described in Ref. 3.

Note that the contributions to the effective supersaturation of the individual components in Eq. (1) are all relatively small; their product gives a value of 2.7 for $\overline{S}$, yielding an unphysically low theoretical nucleation rate of 10^{-44} cm^{-3} s^{-1}. The reason for this remarkable discrepancy is not clear at the moment. The above definition of $\overline{S}$ is easily justified thermodynamically, not only in the semiphenomenological framework of Ref. 3, but also in the classical (capillarity) approximation. In our opinion, there are two arguments that might help explain the large difference.

First, at low supersaturations and intermediate pressures, both semiphenomenological and classical models are known to predict much too low nucleation rates, even for the binary model systems.[3,5,11] Notably at these small values of supersaturation, the sensitivity of nucleation rates on $\overline{S}$ is extreme. Consequently, the numerical value of J depends strongly on the calculated equilibrium fractions. These in their turn depend on the (measured) input fractions and on the equation of state used. For one single experiment, theoretical nucleation rates resulting from SRK or PR equilibrium calculations may differ by as much as ten orders of magnitude, although both are still much too low. As is more often the case in nucleation work, there exists no experimental evidence for the preference of either one of the equations in the range of conditions under study. It is well possible that both of them predict too large equilibrium fractions, so that the supersaturations are significantly too small.

A second—more intuitive—interpretation is the following. Although discrepancies between theory and experiment

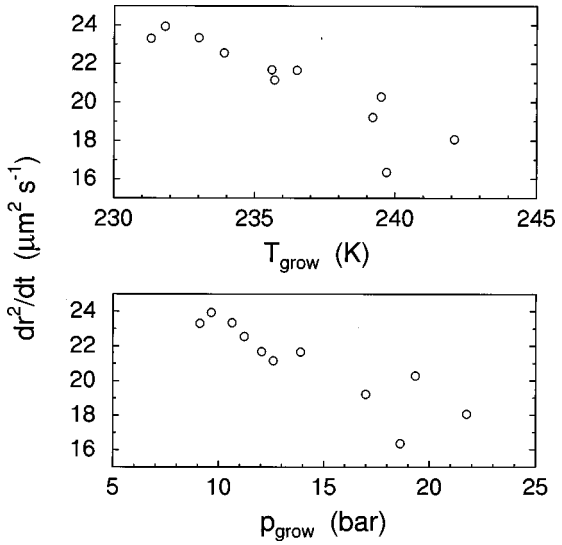

FIG. 5. Experimental droplet growth rates versus growth conditions for natural gas type B.

are not often sought in nucleation kinetics, these might play a role in the present circumstances. Since there is such a large number of components present, there are many possible routes along which stable clusters can be formed (with numerous possible configurations leading to the same energy of formation).[12] Mathematically, this would imply an integration over many coordinates in n_i space, resulting in a very large Zeldovich factor. We have observed that the latter increases by more than an order of magnitude when going from unary to binary nucleation; it is well possible that this increase continues with increasing dimensionality of the nucleating system.

B. Droplet growth

We now turn to the experimental results for droplet growth rates. Most experiments show a linear increase of r_d^2 with time (see Fig. 3), implying diffusion controlled growth. This comes as no surprise in view of the intermediate pressures under consideration, which cause the mean free path to be always much smaller than the droplet radius. For the experiments of series B, the average growth rates dr_d^2/dt have been plotted in Fig. 5 as a function of both pressure and temperature during the growth period (the pressure plateau in Fig. 3).

It can be demonstrated that the expression for diffusion controlled droplet growth in a multicomponent system, in the limit of dilute vapor components in a noncondensing background gas, can be written as

$$\frac{dr_d^2}{dt} = 2\,\frac{\rho_v}{\rho_l}\sum_{i=1}^{n}\mathcal{D}_i(y_i - y_i^{\mathrm{eq}}), \tag{2}$$

provided that the components are well miscible. $\mathcal{D}_i$ denotes the diffusion coefficient of component i in the background gas; ρ_v and ρ_l are the total molar densities of the vapor and liquid phases. The molar fractions y_i and y_i^{eq} are input (feed) and equilibrium fractions of component i, respectively.

The equilibrium fractions and molar densities are again calculated from a suitable equation of state, now applied at the conditions of the growth process: both pressure and temperature during growth are higher than in the nucleation pulse (which is the very basis of the pulse method). Values for our sample experiment are included in Table II. For the diffusion coefficients $\mathcal{D}_i$ we adopted the correlation according to Fuller,[8] thereby assuming diffusion of each component in pure methane gas. For typical growth conditions, the resulting values of $\mathcal{D}_i$ are near 3×10^{-7} m^2 s^{-1}, with only very modest differences between components.

Calculating the expected growth rate for the sample experiment, we arrive at $dr_d^2/dt = 1.79\times10^{-11}$m^2 s^{-1}, whereas the experimental value equals 1.81×10^{-11} m^2 s^{-1}. This remarkable agreement is somewhat lucky; in Table III some other values are given (note that run 307 is our sample experiment). From Table III, the influence of the applied equation of state can also be deduced: the Benedict–Webb–Rubin equation probably gives too low equilibrium fractions, resulting in overestimated growth rates for all experiments. The PR equation seems to do the best job in this respect: growth rates are all reasonably close to the experiment. Apparently, we are indeed dealing with simultaneous growth of all supersaturated components, the dominating substances being the heavier alkane fractions C_7–C_{10} and the aromatics (benzenes).

We are now also able to explain the observed decrease of growth rates in Fig. 5. First, the product of vapor density and diffusion coefficient is fairly insensitive to pressure, since $\mathcal{D}_i \propto \rho_v^{-1}$. The liquid density does not vary much. Direct temperature dependencies are only found in the diffusion coefficients and the equilibrium vapor fractions. Since diffusion coefficients *increase* with temperature—with $T^{1.75}$

TABLE III. Calculational results for growth rates of some selected experiments. Note the strong influence of the applied equation of state (EOS).

Run No.	p_{grow} (bar)	T_{grow} (K)	$(dr_d^2/dt)_{\mathrm{expt.}}$ (10^{-11} m^2 s^{-1})	EOS	ρ_v (mol ℓ^{-1})	ρ_l (mol ℓ^{-1})	$\Sigma_i\mathcal{D}_i(y_i-y_i^{\mathrm{eq}})$ (10^{-11} m^2 s^{-1})	$(dr_d^2/dt)_{\mathrm{model}}$ (10^{-11} m^2 s^{-1})
211	16.9	239.1	1.91	PR	0.914	9.221	11.5	2.28
				SRK	0.904	9.278	13.5	2.63
				BWR	0.905	10.13	18.3	3.27
307	21.8	242.2	1.81	PR	1.185	9.277	7.02	1.79
				BWR	1.171	10.33	10.9	2.48
407	21.8	243.2	1.85	PR	1.180	9.125	6.72	1.74
				BWR	1.166	10.16	11.1	2.56

according to the Fuller correlation—this cannot explain the decreasing growth rate. The solution must therefore be sought in the equilibrium fractions: these are not much smaller than the feed fractions (see Table II). Hence, an increase in growth temperature gives an enhanced equilibrium fraction and a decreasing growth rate. The observed decrease with *pressure* is therefore not a physical effect on its own: it is simply caused by the correlation of experimental temperatures and pressures along isonucleation curves (see Fig. 4).

IV. CONCLUSIONS

We have presented the first quantitative experimental investigation of the condensation behavior of a multicomponent mixture: dry natural gas, consisting mainly of methane, nitrogen, and a large number of heavier hydrocarbons. This study was initiated from an interest in both the question of the possibility of such measurements, and the industrial call for experimental data on natural gas condensation.

Nucleation and droplet growth rates were measured using the pulse-expansion wave tube technique, at realistic pressures for natural gas handling. Optical measurement of the time-resolved droplet radius using Mie scattering turned out to be very well possible, with no important differences with respect to unary or binary systems. The same holds for the determination of droplet number densities (hence, nucleation rates) by means of extinction measurement.

Special care was taken in the preparation of the test mixture. In order to preserve the original vapor composition, pressure drops were avoided by isobarically dispelling nitrogen from the test section. In this way, the total volume of the test section was flushed three times before each experiment. This procedure was first tested; in addition, some experiments were performed with sixfold flushing, without noticeable difference.

Plotting the nucleation data in the (p,T) diagram, experimental isonucleation curves are found that correspond to the behavior that is expected from model calculations for binary mixtures of methane with one heavier alkane. The latter comprise computations of nucleation rates using binary classical nucleation theory, including real gas thermodynamics for which the SRK equation of state is used. Particularly, for a mixture of *n*-octane (molar fraction 5×10^{-4}) and methane, the behavior is even quantitatively comparable. However, this fact should only be regarded as a convenient interpolation tool, since the model calculations do not quantitatively reproduce experimental observations for the binary mixture itself.

Comparison of the data to an existing multicomponent nucleation model shows very large discrepancies; we have suggested possible reasons. The most important of these is the essential role of equilibrium calculations, which are always based on extrapolations for the circumstances under study. Consequently, predicted nucleation rates are very sensitive to the equation of state applied and to the input composition. An alternative suggestion concerns nucleation kinetics: probably, the kinetic prefactor in the multicomponent nucleation model is too low since it is based on effective one-component kinetics. This approach discards the fact that there are many possible routes to form a cluster with a given free energy in a multidimensional particle space.

Droplet growth is found to be diffusion controlled: The droplet radius squared increases linearly with time in most cases. The average droplet growth rates dr_d^2/dt are compared to a multicomponent model for diffusion controlled growth. The agreement is satisfactory, but does depend on the equation of state that is used to calculate the equilibrium vapor fractions. The observation that the growth rate decreases with growth temperature has been explained from the temperature dependence of these equilibrium vapor fractions.

[1] Y. Viisanen and R. Strey, J. Chem. Phys. **105**, 8293 (1996).
[2] M. J. E. H. Muitjens, V. I. Kalikmanov, M. E. H. van Dongen, A. Hirschberg, and P. Derks, Rev. Inst. Fr. Pet. **49**, 63 (1994).
[3] V. I. Kalikmanov and M. E. H. van Dongen, Phys. Rev. E **55**, 1607 (1997).
[4] K. N. H. Looijmans, P. C. Kriesels, and M. E. H. van Dongen, Exp. Fluids **15**, 61 (1993).
[5] K. N. H. Looijmans, C. C. M. Luijten, and M. E. H. van Dongen, J. Chem. Phys. **103**, 1714 (1995).
[6] K. N. H. Looijmans and M. E. H. van Dongen, Exp. Fluids **23**, 54 (1997).
[7] C. C. M. Luijten, K. J. Bosschaart, and M. E. H. van Dongen, J. Chem. Phys. **106**, 8116 (1997).
[8] R. C. Reid, J. M. Prausnitz, and B. E. Poling, *The Properties of Gases and Liquids*, 4th ed. (McGraw–Hill, New York, 1987).
[9] The magnitude of this shift is comparable to the mutual distance between the envelopes of different cylinder types: hence, the choice of equation of state introduces an uncertainty in equilibrium data that is of the same order as that resulting from the composition differences.
[10] K. N. H. Looijmans, C. C. M. Luijten, G. C. J. Hofmans, and M. E. H. van Dongen, J. Chem. Phys. **102**, 4531 (1995).
[11] K. N. H. Looijmans, Ph. D. thesis, Eindhoven University of Technology, TUE Eindhoven, 1995.
[12] The multicomponent model uses effective one-component nucleation kinetics, resulting in a Zeldovich factor that is typical for unary nucleation.